

Coupled-resonator-induced reflection in photonic-crystal waveguide structures

Sergei F. Mingaleev¹, Andrey E. Miroschnichenko²,
and Yuri S. Kivshar²

¹ VPI Development Center, Belarus High Technologies Park, Minsk 220034, Belarus

² Nonlinear Physics Center and Center for Ultra-high bandwidth Devices for Optical Systems (CUDOS), Australian National University, Canberra ACT 0200, Australia

Abstract: We study the resonant transmission of light in a coupled-resonator optical waveguide interacting with two nearly identical side cavities. We reveal and describe a novel effect of the coupled-resonator-induced reflection (CRIR) characterized by a very high and easily tunable quality factor of the reflection line, for the case of the inter-site coupling between the cavities and the waveguide. This effect differs sharply from the coupled-resonator-induced transparency (CRIT) – an all-optical analogue of the electromagnetically-induced transparency – which has recently been studied theoretically and experimentally for the structures based on micro-ring resonators and photonic crystal cavities. Both CRIR and CRIT effects have the same physical origin which can be attributed to the Fano-Feshbach resonances in the systems exhibiting more than one resonance. We discuss the applicability of the novel CRIR effect to the control of the slow-light propagation and low-threshold all-optical switching.

© 2008 Optical Society of America

OCIS codes: (230.7390) Waveguides, planar; (260.2030) Dispersion; (250.5300) Photonic integrated circuits; (230.5750) Resonators; (999.9999) Photonic crystals, (999.9999) Group Velocity.

References and links

1. B. E. Little, S. T. Chu, H. A. Haus, J. Foresi, and J.-P. Laine, "Microring resonator channel dropping filters," *J. Lightwave Technol.* **15**, 998–1005 (1997).
2. S. Fan, P. R. Villeneuve, J. D. Joannopoulos, M. J. Khan, C. Manolatou, and H. A. Haus, "Theoretical analysis of channel drop tunneling processes," *Phys. Rev. B* **59**, 15882–15892 (1999).
3. Y. Xu, Y. Li, R. K. Lee, and A. Yariv, "Scattering-theory analysis of waveguide-resonator coupling," *Phys. Rev. E* **62**, 7389–7404 (2000).
4. D. D. Smith, H. Chang, K. A. Fuller, A. T. Rosenberger, and R. W. Boyd, "Coupled-resonator-induced transparency," *Phys. Rev. A* **69**, 063804 (2004).
5. D. D. Smith and H. Chang, "Coherence phenomena in coupled optical resonators," *J. Mod. Opt.* **51**, 2503–2513 (2004).
6. L. Maleki, A. B. Matsko, A. A. Savchenkov, and V. S. Ilchenko, "Tunable delay line with interacting whispering-gallery-mode resonators," *Opt. Lett.* **29**, 626–628 (2004).
7. A. B. Matsko, A. A. Savchenkov, D. Strelakov, V. S. Ilchenko and L. Maleki, "Interference effects in lossy resonator chains," *J. Mod. Opt.* **51**, 2515–2522 (2004).
8. W. Suh, Z. Wang, and S. Fan, "Temporal coupled-mode theory and the presence of non-orthogonal modes in lossless multimode cavities," *IEEE J. Quantum Electron.* **40**, 1511–1518 (2004).
9. T. Opatrny and D. G. Welsch, "Coupled cavities for enhancing the cross-phase-modulation in electromagnetically induced transparency," *Phys. Rev. A* **64**, 23805 (2001).
10. A. Naweed, G. Farca, S. I. Shopova, and A. T. Rosenberger, "Induced transparency and absorption in coupled whispering-gallery microresonators," *Phys. Rev. A* **71**, 043804 (2005).
11. Q. Xu, S. Sandhu, M. L. Povinelli, J. Shakya, S. Fan, and M. Lipson, "Experimental realization of an on-chip all-optical analogue to electromagnetically induced transparency," *Phys. Rev. Lett.* **96**, 123901 (2006).

12. Q. Xu, J. Shakya, and M. Lipson, "Direct measurement of tunable optical delays on chip analogue to electromagnetically induced transparency," *Opt. Express* **14**, 6463–6468 (2006).
13. J. Pan, S. Sandhu, Y. Huo, M. L. Povinelli, M. M. Fejer, S. Fan, and J. S. Harris, "Optical Analogue to Electromagnetically Induced Transparency in Photonic Crystals, Simulation and Experiments," in *Slow and Fast Light*, OSA Technical Digest (CD) (Optical Society of America, 2007), paper SWB2. <http://www.opticsinfobase.org/abstract.cfm?URI=SL-2007-SWB2>
14. R. W. Boyd and D. J. Gauthier, "Transparency on an optical chip," *Nature* **441**, 701–702 (2006).
15. B. Maes, P. Bienstman, and R. Baets, "Switching in coupled nonlinear photonic-crystal resonators," *J. Opt. Soc. Am. B* **22**, 1778–1784 (2005).
16. S. F. Mingaleev, A. E. Miroshnichenko, Y. S. Kivshar, and K. Busch, "All-optical switching, bistability, and slowlight transmission in photonic crystal waveguide-resonator structures," *Phys. Rev. E* **74**, 046603 (2006).
17. S. F. Mingaleev, A. E. Miroshnichenko, and Y. S. Kivshar, "Low-threshold bistability of slow light in photonic-crystal waveguides," *Opt. Express* **15**, 12380–12385 (2007).
18. S. Fan, "Manipulating light with photonic crystals," *Physica B* **394**, 221–228 (2007).
19. S. Fan, "Sharp asymmetric line shapes in side-coupled waveguide-cavity systems," *Appl. Phys. Lett.* **80**, 908–910 (2002).
20. A. E. Miroshnichenko, S. F. Mingaleev, S. Flach, and Y. S. Kivshar, "Nonlinear Fano resonance and bistable wave transmission," *Phys. Rev. E* **71**, 036626 (2005).
21. M. F. Yanik and S. Fan, "Stopping light all optically," *Phys. Rev. Lett.* **92**, 083901 (2004).
22. A. Yariv, Y. Xu, R. K. Lee, and A. Scherer, "Coupled-resonator optical waveguide: a proposal and analysis," *Opt. Lett.* **24**, 711 (1999).
23. K. Busch, S. F. Mingaleev, A. Garcia-Martin, M. Schillinger, and D. Hermann, "Wannier function approach to photonic crystal circuits," *J. Phys.: Condens. Matter.* **15**, R1233–R1256 (2003).
24. S. G. Johnson and J. D. Joannopoulos, "Block-iterative frequency-domain methods for Maxwell's equations in a planewave basis," *Opt. Express* **8**, 173–190 (2001).
25. H. Feshbach, "Unified theory of nuclear reactions, I," *Ann. Phys. (N.Y.)* **5**, 357 (1958); "A unified theory of nuclear reactions, II," *Ann. Phys. (N.Y.)* **19**, 287 (1962).
26. F. H. Mies, "Configuration interaction theory: effects of overlapping resonances," *Phys. Rev.* **175**, 164–175 (1968); F. H. Mies, "Resonant scattering theory of association reactions and unimolecular decomposition: I. A united theory of radiative and collisional recombination," *J. Chem. Phys.* **51**, 787–797 (1969).
27. A. I. Magunov, I. Rotter, and S. I. Strakhova, "Fano resonances in the overlapping regime," *Phys. Rev. B* **68**, 245305 (2003).
28. M. Raouf and F. H. Mies, "Feshbach resonance in atomic binary collisions in the wigner threshold law regime," *Phys. Rev. A* **70**, 012710 (2004).
29. L. Y. Mario, S. Darmawan, and M. K. Chin, "Asymmetric Fano resonance and bistability for high extinction ratio, large modulation depth, and low power switching," *Opt. Express* **14**, 12770–12781 (2006).
30. Y. A. Vlasov, M. O'Boyle, H. F. Hamann, and S. J. McNab, "Active control of slow light on a chip with photonic crystal waveguides," *Nature* **438**, 65–69 (2005).
31. H. Gersen, T. J. Karle, R. J. P. Engelen, W. Bogaerts, J. P. Korterik, N. F. van Hulst, T. F. Krauss, and L. Kuipers, "Direct observation of Bloch harmonics and negative phase velocity in photonic crystal waveguides," *Phys. Rev. Lett.* **94**, 123901 (2005).
32. M. Notomi, K. Yamada, A. Shinya, J. Takahashi, C. Takahashi, and I. Yokohama, "Extremely large group velocity dispersion of line-defect waveguides in photonic crystal slabs," *Phys. Rev. Lett.* **87**, 253902 (2001).
33. R. Jacobsen, A. Lavrinenko, L. Frandsen, C. Peucheret, B. Zsigri, G. Moulin, J. Fage-Pedersen, and P. Borel, "Direct experimental and numerical determination of extremely high group indices in photonic crystal waveguides," *Opt. Express* **13**, 7861–7871 (2005).
34. S. Assefa, S. J. McNab, and Y. A. Vlasov, "Transmission of slow light through photonic crystal waveguide bends," *Opt. Lett.* **31**, 745–747 (2006).
35. Y. A. Vlasov and S. J. McNab, "Coupling into the slow light mode in slab-type photonic crystal waveguides," *Opt. Lett.* **31**, 50–52 (2006).

1. Introduction

Many concepts of photonic devices employ high- Q optical resonators, such as micro-rings or photonic crystal cavities, side coupled to the transmission waveguide. Among them, the devices which employ *several resonators* have attracted a special attention because the coupling between optical resonators may lead to a variety of novel effects such as the high-order resonances with flattened passband region [1, 2, 3], the appearance of additional resonances with extremely high- Q factors [3], etc. One of the most interesting and promising effects that was discovered for the double-resonator photonic structure shown schematically in Fig. 1(a) is an all-

optical analogue of the *electromagnetically-induced transparency* (EIT). We describe the resonant transmission observed for such structure as the effect of *coupled-resonator-induced transparency* (CRIT) [4]. It has been predicted theoretically by several research groups [4, 5, 6, 7, 8], although one can also mention the early work [9] which suggested an idea of *macroscopic* double-resonator optical system exhibiting the same EIT-like effect. Recently, the CRIT effect has been observed experimentally in the system of two interacting micro-resonators for the whispering-gallery modes [10] and in the integrated photonic chips employed either two micro-ring resonators [11, 12] or two photonic-crystal cavities [13]. Such CRIT devices provide an efficiently tunable ‘transparency on an optical chip’, and they are considered as a crucial step towards the development of integrated all-optical chips [14]. In particular, they can be employed for significant (10^3 times) reduction of the threshold power for optical bistability [15].

In this paper, we study the transmission of light in several types of the resonant structures based on a photonic-crystal (PhC) waveguide side-coupled to two nearly identical PhC cavities, as shown schematically in Fig. 1(b) and Fig. 1(c). We confirm that in the case of *on-site* coupling of two cavities to a PhC waveguide, as shown schematically in Fig. 1(b), the CRIT effect may be observed (see also the recent experimental observation [13] of the CRIT effect in a PhC structure with on-site coupling). However, for the structure shown in Fig. 1(c), we reveal the existence of a closely related effect of *coupled-resonator-induced reflection* (CRIR) that manifests itself in an extremely narrow resonant reflection line whose quality factor can easily be tuned by changing one of the cavities. Specifically, the quality factor grows indefinitely when the optical properties of two coupled cavities become identical.

In a sharp contrast to the CRIT effect that can be observed in the structures with many different types of waveguides [11, 12, 13] or even for light propagating in free space with no waveguide at all [10], we reveal that the existence of the CRIR effect is determined by the *discrete nature* of the photonic crystal waveguide and it can be observed, therefore, in either coupled-resonator optical waveguides (CROWs) or PhC waveguides, both created by an array of coupled optical cavities. Recently, we have demonstrated a crucial importance of the discrete nature of PhC waveguides for achieving high- Q resonant reflection and low-threshold all-optical switching in the slow-light regime [16, 17]. We have shown that this can be achieved by employing of *inter-site coupling* of a single Kerr nonlinear cavity to a PhC waveguide.

Here, we extend those results further and demonstrate that employing of *inter-site coupling* of *two cavities* in the PhC waveguide structure shown schematically in Fig. 1(c), leads to the transformation of the CRIT effect into the CRIR effect. We also show that in contrast to the CRIT effect in the structures with the on-site coupling, the CRIR effect observed in the structures with the inter-site coupling *survives in the slow-light regime*, and thus it can be employed for a control on the slow-light propagation and switching. As an example, we demonstrate a possibility to achieve 100% all-optical switching of slow light in the nonlinear regime.

2. Coupled-resonator-induced transparency

First, we remind the basic facts about the CRIT effect assuming for definiteness that the resonant photonic structure is created by a straight dielectric waveguide and two side-coupled cavities, denoted as α and β and separated by the distance d along waveguide, as shown schematically in Fig. 1(a).

To simplify the analysis, below we assume that any losses are absent, so that the transmission ($T(\omega)$) and reflection ($R(\omega)$) coefficients can be conveniently written in the form

$$T(\omega) = \frac{\sigma^2(\omega)}{\sigma^2(\omega) + 1} \quad , \quad R(\omega) = \frac{1}{\sigma^2(\omega) + 1} \quad , \quad (1)$$

where the detuning function $\sigma(\omega)$ may have a rather general frequency dependence defined by

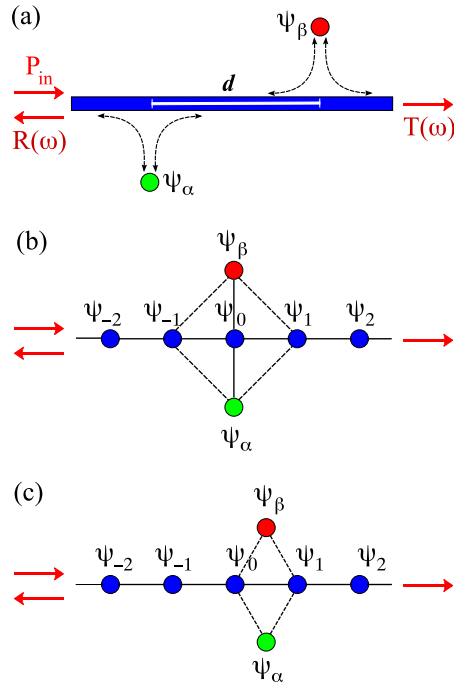


Fig. 1. Three types of the geometries of a straight photonic-crystal waveguide side coupled to two nonlinear optical resonators, α and β . Standard coupled-mode theory is based on the geometry (a) which does not account for discreteness-induced effects in the photonic-crystal waveguides. For instance, light transmission and bistability are qualitatively different for (b) on-site and (c) inter-site locations of the resonator along waveguide and this cannot be distinguished within the conceptual framework of structure of type (a).

the type of the PhC waveguide-cavity structures (see, e.g., several examples in Refs. [16, 20]). The zero transmission (complete reflection) corresponds to the condition $\sigma(\omega) = 0$, whereas the complete transmission (vanishing reflection) corresponds to the condition $\sigma(\omega) = \pm\infty$. Therefore, the resonant frequencies can be conveniently found as zeros of the nominator and denominator of the auxiliary function $\sigma(\omega)$.

For the simplest resonant structure created by a straight waveguide coupled to a single cavity (e.g., the cavity α), we can obtain [16]

$$\sigma(\omega) \simeq \frac{(\omega_\alpha - \omega)}{\gamma_\alpha}, \quad (2)$$

with a resonant reflection at the frequency that almost coincides with the frequency ω_α of the localized cavity mode of an isolated cavity. The spectral width γ_α of the resonance is determined by the overlap integral between the cavity mode and the waveguide mode at the resonant frequency, rapidly decaying as the distance between the cavity and the waveguide grows.

To find the characteristic function $\sigma(\omega)$ for the waveguide structure with two cavities, we can employ a variety of methods [5, 6, 7, 8, 15], including the simplest approach based on the transfer-matrix technique [19]. A detailed analysis of the light scattering in such structures can be found in Refs. [6, 11, 18], and here we present the results for the special case when two cavities are separated by the distance $d = 2\pi m/k(\omega_t)$, where $k(\omega)$ is the waveguide dispersion

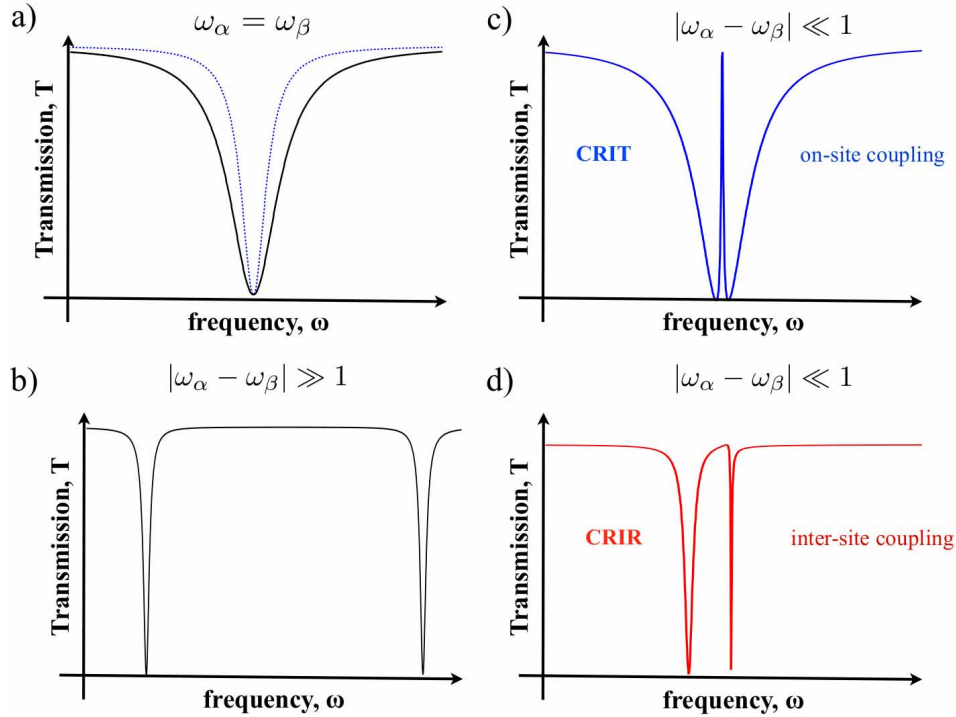


Fig. 2. Typical transmission curves for four different cases (a) two identical side-coupled defects $\omega_\alpha = \omega_\beta$ (solid). For reference we also put transmission for single side-coupled cavity (dashed); (b) two side-coupled cavities with larger detuned eigenfrequencies $|\omega_\alpha - \omega_\beta| \gg 1$; (c) and (d) correspond to two side-coupled cavities with slightly detuned eigenfrequencies $|\omega_\alpha - \omega_\beta| \ll 1$ for two geometries: (c) on-site coupling shown in Fig. 1(b) and (d) inter-site coupling shown in Fig. 1(c).

relation, m is integer, and the frequency ω_t is defined below. In this case, assuming that there is no direct coupling between the cavities, i.e. either the distance d is sufficiently large or the cavities are coupled to the waveguide from the opposite sides, we obtain

$$\sigma(\omega) \simeq \frac{(\omega_\alpha - \omega)(\omega_\beta - \omega)}{\Gamma(\omega_t - \omega)}, \quad (3)$$

with the total resonance width $\Gamma = \gamma_\alpha + \gamma_\beta$ and the frequency of perfect transmission

$$\omega_t = \frac{\gamma_\alpha \omega_\beta + \gamma_\beta \omega_\alpha}{\gamma_\alpha + \gamma_\beta}, \quad (4)$$

lying in between the two frequencies, ω_α and ω_β , of the zero transmission. Importantly, these frequencies coincide with the frequencies of the localized cavity modes of the isolated cavities α and β .

In the case when the cavities α and β are identical, Eq. (3) reduces to the single-cavity result (2) with a doubled resonance width, $\Gamma = 2\gamma_\alpha$, as is illustrated in Fig. 2(a). When the cavities α and β are significantly different, the structure exhibits two almost uncoupled single-cavity resonances, as is illustrated in Fig. 2(b). However, introducing only a *small* difference between the parameters of the two cavities leads to opening an extremely narrow resonant

transmission on the background of the broader reflection line, as is illustrated in Fig. 2(c). Indeed, for a small difference between the cavity parameters we assume that $\gamma_\beta \approx \gamma_\alpha$, and introducing notation $\delta\omega = \omega_\beta - \omega_\alpha$, rewrite Eq. (3) in the vicinity of the resonant transmission frequency as $\sigma(\omega) \approx \Gamma_t/(\omega - \omega_t)$ with $\omega_t = \omega_\alpha + \delta\omega/2$ and

$$\Gamma_t = \delta\omega^2/8\gamma_\alpha. \quad (5)$$

The line width Γ_t of this resonance can easily be controlled by tuning the frequency difference $\delta\omega$, and the corresponding quality factor, $Q_t = \omega_t/2\Gamma_t \approx 4\gamma_\alpha\omega_\alpha/\delta\omega^2$, grows indefinitely when $\delta\omega$ vanishes. As we mentioned above, this effect can be regarded as an all-optical analogue of the electromagnetically-induced transparency, and it is now often referred as the effect of *coupled-resonator-induced transparency* – CRIT [4].

3. Model description of photonic crystal structures

For the photonic structures based on photonic-crystal waveguides we have a new option (comparing with strip-waveguide structures) for achieving the resonant transmission by placing the cavity at different location relative to the waveguide and thus exploring the *discrete nature* of the structure. Recently, we have demonstrated [16, 17] that, by employing this extra degree of freedom in the waveguide-cavity geometry with one cavity, we can dramatically increase the quality factor of the resonant reflection in the slow-light regime and, accordingly, decrease the light power required for the observation of bistability in the light transmission. Here, we extend this analysis to the case of two-cavity structures and reveal new physics.

As was shown in Refs. [16, 20], the light transmission in the waveguide-cavity photonic crystal structures can be accurately modeled with the effective discrete equations for the frequency-dependent dimensionless electric field amplitudes of the cavity modes composing the waveguide, $\psi_n(\omega)$, with integer $n \in [-\infty, \infty]$, and side-coupled cavity modes, $\psi_\mu(\omega)$, with $\mu = \alpha, \beta$. By applying this approach to the structures shown in Figs. 1(b,c), such equations can be rewritten as follows

$$\begin{aligned} \rho(\omega)\psi_n &= \psi_{n+1} + \psi_{n-1} + \sum_{\mu=\alpha,\beta} \eta_{n,\mu} \psi_\mu, \\ \frac{(\omega - \omega_\mu)}{\gamma_\mu^{(0)}} \psi_\mu &= \sum_{n=-\infty}^{\infty} \eta_{n,\mu} \psi_n + \lambda_\mu |\psi_\mu|^2 \psi_\mu. \end{aligned} \quad (6)$$

Here, $\rho(\omega) = 2 \cos[k(\omega)s]$, where $k(\omega)$ describes the waveguide dispersion and s is the distance between nearest-neighboring waveguide's cavities. Each side-coupled cavity μ is described by the frequency ω_μ of the localized cavity mode, the dimensionless Kerr nonlinearity coefficient λ_μ , and the “effective” spectral width $\gamma_\mu^{(0)}$ of the single-cavity resonance (the meaning of “effective” here will be clarified in the subsequent analysis). The dimensionless coupling coefficients $\eta_{n,\mu}$ are assumed to be equal (after appropriate rescaling of ψ_μ , $\gamma_\mu^{(0)}$, and λ_μ) to either zero or ± 1 ; their values will be indicated in what follows individually for each studied case. The resonance detuning function $\sigma(\omega)$ can be found by solving Eq. (6) in the way similar to that described in Refs. [16, 20].

These equations are valid in the approximation of local coupling between the cavities composing the waveguide structure which has been shown to produce qualitatively (and even semi-quantitatively) correct results [16, 20]. In the form (6), the effective discrete equations look very similar to those derived from the coupled-mode theory [21] for the case of coupled-resonator optical waveguides [22] and, therefore, our subsequent analysis can be applied to all such structures as well.

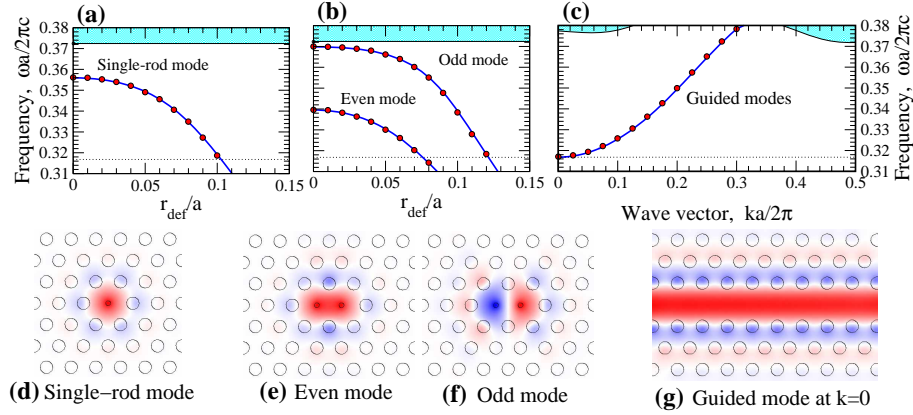


Fig. 3. Frequencies of localized cavity modes created by changing the radius r_{def} of (a) a single rod [with the electric field profile of the mode shown in (d)], and (b) two neighboring rods [with the electric field profiles of two modes shown in (e) and (f)] in the photonic crystal created by a triangular lattice of rods with $\epsilon = 12$ and radius $r = 0.25a$ in air, a is the lattice spacing. (c) Dispersion of the W1 photonic-crystal waveguide created by removing a row of rods in the same photonic crystal [with the electric field profile of the slow-light guided mode at the propagation band edge $k = 0$ shown in (g)]. Results are calculated with eleven maximally localized Wannier functions[23] (blue lines) in an excellent agreement with the supercell plane-waves method [24] (red circles).

First, we analyze briefly the photonic crystal structure with two cavities, α and β , side-coupled to the same *on-site location* along PhC waveguide as shown in Fig. 1(b). The situation when only one of these cavities is coupled to the waveguide (with $\eta_{n,\alpha} = \delta_{n,0}$ and $\eta_{n,\beta} = 0$, where $\delta_{n,m}$ is the Kronecker symbol) has already been studied earlier in Refs. [16, 20]. In this case the model parameters introduced in Eq. (6) are related to the parameters introduced in Eqs. (21)–(24) of Ref. [16] as $\psi_n \equiv A_n$, $\Psi_\alpha \equiv (V_{0,\alpha}/V_{1w})A_\alpha$, $\gamma_\alpha^{(0)} = v_\alpha \omega_\alpha V_{0,\alpha} V_{\alpha,0}/V_{1w}$, and $\lambda_\alpha = (\kappa_\alpha \chi_\alpha^{(3)}/V_{\alpha,0})(V_{1w}/V_{0,\alpha})^3$. Therefore, the linear (at $\lambda_\alpha = 0$) detuning function $\sigma(\omega)$ found for this case in Ref. [16] takes the form of Eq. (2) with unchanged form of ω_α and with $\gamma_\alpha = \gamma_\alpha^{(0)}/\sin[k(\omega_\alpha)s]$. As one can see, $\gamma_\alpha^{(0)}$ is the spectral width of the resonant reflection line that would be produced by a single on-site side-coupled cavity in the case when its frequency ω_α lies at the center of the waveguide transmission band, $k(\omega_\alpha) = \pi/2s$.

In the same way, we can show that the detuning function of the on-site two-cavity structure with $\eta_{n,\mu} = \delta_{n,0}$ for both μ , shown in Fig. 1(b), takes the form of Eqs. (3)–(5) with unchanged forms of ω_α and ω_β , and with $\gamma_\alpha = \gamma_\alpha^{(0)}/\sin[k(\omega_\alpha)s]$ and $\gamma_\beta = \gamma_\beta^{(0)}/\sin[k(\omega_\beta)s]$. Correspondingly, this *on-site two-cavity structure exhibits the same effect of coupled-resonator-induced transparency*, illustrated in Fig. 2(c), as discussed in the previous section.

4. Coupled-resonator-induced reflection

Now let us analyze an alternative photonic crystal structure with two cavities, α and β , side-coupled to the same *inter-site location* along PhC waveguide as shown in Fig. 1(c). In this case, $\eta_{n,\mu} = (\delta_{n,0} \pm \delta_{n,1})$, where the upper sign in “ \pm ” corresponds to the even-symmetry cavity modes, while the bottom sign corresponds to the odd-symmetry cavity modes.

The situation when only one of the cavities (say, the cavity α) is coupled to the waveguide (with $\eta_{n,\alpha} = (\delta_{n,0} \pm \delta_{n,1})$, but $\eta_{n,\beta} = 0$) has already been studied for the even-symmetry cavity modes in Refs. [16, 20]. Extending those results to the case of both even- and odd-symmetry

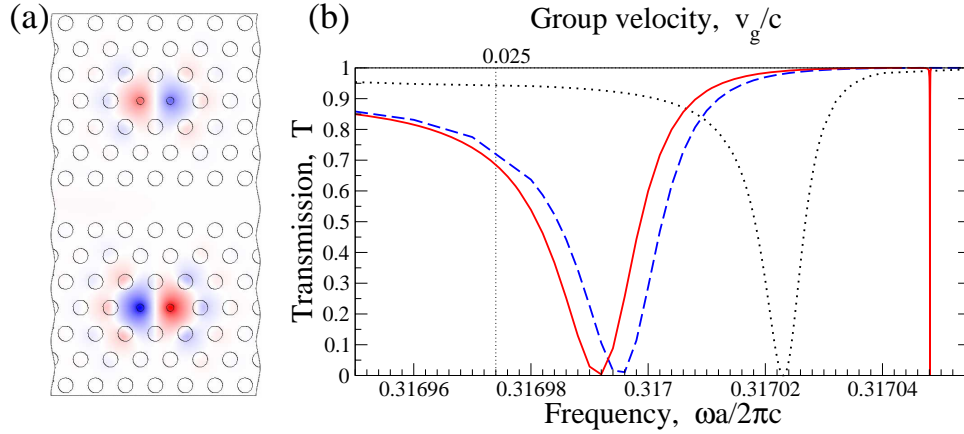


Fig. 4. (a) Schematic structure of a photonic-crystal waveguide coupled to two side cavities. (b) Linear transmission coefficient of the photonic-crystal waveguide for: (i) single side-coupled cavity with $\varepsilon_\alpha = 12$. (dotted); (ii) two identical side-coupled cavities with $\varepsilon_\alpha = \varepsilon_\beta = 12$. (dashed); (iii) two side-coupled cavities with different permittivities $\varepsilon_\alpha = 12$. and $\varepsilon_\beta = 12.001$ (solid).

cavity modes, the detuning parameter for the inter-site single-cavity structure can be obtained in the form

$$\sigma(\omega) \simeq \frac{(\tilde{\omega}_\alpha^\pm - \omega)}{\gamma_\alpha^\pm}, \quad (7)$$

where the resonant reflection frequency $\tilde{\omega}_\alpha^\pm = \omega_\alpha \mp \gamma_\alpha^{(0)}$ is shifted to one or the other side from the frequency ω_α of the cavity mode, depending on its symmetry. The spectral width $\gamma_\alpha^\pm = \gamma_\alpha^{(0)} / [\tan(k(\tilde{\omega}_\alpha^\pm)s/2)]^{\pm 1}$ of this resonance line equals to $\gamma_\alpha^{(0)}$ at the center of waveguide pass-band, but it vanishes at one of the band edges, giving birth to *extremely high-quality resonant reflection lines in the slow-light regime* [16, 17].

For the problem of the light transmission in the inter-site two-cavity structure shown in Fig. 1(c), we solve Eq. (6) and obtain the detuning parameter in the form,

$$\sigma(\omega) \simeq \frac{(\omega_{r1}^\pm - \omega)(\omega_{r2}^\pm - \omega)}{\Gamma^\pm(\omega_t - \omega)}, \quad (8)$$

that looks qualitatively similar to Eq. (3). Moreover, the frequency ω_t of the perfect transmission is determined by the same equation for the CRIT effect (4) with $\gamma_\mu = \gamma_\mu^{(0)}$. However, now the total resonance width $\Gamma^\pm = [\tan(k(\omega_t)s/2)]^{\mp 1} (\gamma_\alpha^{(0)} + \gamma_\beta^{(0)})$ depends on the waveguide dispersion, $k(\omega_t)$, at the resonance frequency leading to the same enhancement of the resonance quality factor at one of the edges of waveguide pass-band as obtained above for the inter-site one-cavity structure. More importantly, the resonant reflection frequencies,

$$\begin{aligned} \omega_{r1}^\pm &= \frac{\omega_\alpha + \omega_\beta}{2} \mp \frac{\gamma_\alpha^{(0)} + \gamma_\beta^{(0)}}{2} \\ &+ \frac{1}{2} \sqrt{(\omega_\alpha - \omega_\beta \mp \gamma_\alpha^{(0)} \pm \gamma_\beta^{(0)})^2 + 4\gamma_\alpha^{(0)}\gamma_\beta^{(0)}}, \\ \omega_{r2}^\pm &= \frac{\omega_\alpha + \omega_\beta}{2} \mp \frac{\gamma_\alpha^{(0)} + \gamma_\beta^{(0)}}{2} \end{aligned}$$

$$- \frac{1}{2} \sqrt{(\omega_\alpha - \omega_\beta \mp \gamma_\alpha^{(0)} \pm \gamma_\beta^{(0)})^2 + 4\gamma_\alpha^{(0)}\gamma_\beta^{(0)}}, \quad (9)$$

do not coincide with the cavity-mode frequencies ω_α and ω_β . Moreover, these two resonant reflection frequencies are always separated by a finite distance exceeding the value $2\sqrt{\gamma_\alpha^{(0)}\gamma_\beta^{(0)}}$ and, therefore, the existence of a narrow resonant transmission becomes merely impossible.

In contrast, the inter-coupling between the waveguide and two cavities in this system manifests itself in a *qualitatively new effect* of coupled-resonator-induced reflection: for small $\delta\omega = \omega_\beta - \omega_\alpha$ one of the resonant reflection frequencies moves very close to the perfect transmission frequency, ω_t , producing a *narrow resonant reflection line*, as is illustrated in Fig. 2(d). The frequency of this line is always close to the frequency ω_α of the cavity mode, while its spectral width is determined by the frequency difference $\delta\omega$ growing indefinitely as $\delta\omega$ vanishes. For a small difference between the cavity frequencies, assuming $\gamma_\beta^{(0)} \approx \gamma_\alpha^{(0)}$, we can estimate that the spectral width of this narrow reflection line is

$$\begin{aligned} \Gamma_r^\pm &= [\tan(k(\omega_t)s/2)]^{\mp 1} \gamma_\alpha^{(0)} \left(1 - 1/\sqrt{1 + (\delta\omega/2\gamma_\alpha^{(0)})^2} \right) \\ &\approx [\tan(k(\omega_t)s/2)]^{\mp 1} \delta\omega^2/8\gamma_\alpha^{(0)}, \end{aligned} \quad (10)$$

At small $\delta\omega$ and ω_t lying at the center of the passing band, this spectral width almost coincides with the corresponding width (5) of the narrow resonant transmission line in the structures exhibiting the CRIT effect.

In addition to this narrow resonant reflection line, there always exists the second resonant reflection line located (at small $\delta\omega$) at the frequency $\omega_r^\pm = \omega_\alpha \mp 2\gamma_\alpha^{(0)}$, significantly shifted from the frequency of the cavity modes. This line is characterized by the spectral width $\Gamma^\pm = 2\gamma_\alpha^{(0)} [\tan(k(\omega_t)s/2)]^{\mp 1}$ which is twice larger than the width of the corresponding single-cavity resonance [16].

It should be emphasized that despite such a qualitative difference in their spectral manifestations, both CRIT and CRIR effects have the same physical origin which can be attributed to the Fano-Feshbach resonances [25, 26] known to originate from the interaction of two or more resonances (e.g., two Fano resonances) in the overlapping regime where the spectral widths of the resonances are comparable to or larger than the frequency separation between them. In a general case, this leads to a drastic deformation of the transmission spectrum and the formation of additional resonances with sharp peaks. The Fano-Feshbach resonances are associated with a collective response of multiple interacting resonant degrees of freedom, and they have numerous evidences in quantum mechanical systems [27, 28].

For the PhC structures studied in this paper, the two resonant degrees of freedom are associated with two side-coupled cavities, which can be coupled to PhC waveguide in two different ways, illustrated in Fig. 1(b) and Fig. 1(c), with the different manifestation of the Fano-Feshbach resonance in these two cases in the form of either CRIT or CRIR effects.

5. Alternative two-cavity structures

The transmission spectra that look similar to the CRIR spectrum presented in Fig. 2(d) have already been observed in other types of two-cavity photonic structures such as the two-ring resonators [29] where one ring is coupled to both input and output waveguides and the second ring is coupled to the first ring only. It is important, therefore, to clarify a relation between the asymmetric Fano resonances in such structures and the CRIR effect discussed here.

Our analysis shows that the transmission properties of the two-ring structure studied in Ref. [29] are qualitatively the same as the properties of the photonic-crystal structure with

one cavity, say α , side-coupled to the PhC waveguide and the second cavity, say β , coupled to the first cavity only. The light transmission in such structures may be studied with the discrete equations similar to Eqs. (6). Assuming the on-site coupling of the cavity α to the waveguide, for such a structure we obtain the following detuning function

$$\sigma(\omega) \simeq \frac{(\omega_r^+ - \omega)(\omega_r^- - \omega)}{\gamma_\alpha(\omega_t - \omega)}, \quad (11)$$

where $\gamma_\alpha = \gamma_\alpha^{(0)} / \sin[k(\omega_\alpha)s]$, the frequency of the perfect transmission coincides with the frequency of the localized mode of the second cavity, $\omega_t \equiv \omega_\beta$, and the two frequencies of zero transmission are determined by the expressions:

$$\omega_r^\pm = \frac{\omega_\alpha + \omega_\beta}{2} \pm \frac{1}{2} \sqrt{(\omega_\alpha - \omega_\beta)^2 + 4\gamma_{\alpha,\beta}^2}, \quad (12)$$

where the constant $\gamma_{\alpha,\beta}$ determines the coupling between the cavities α and β .

A straightforward analysis of the transmission spectrum in such a structure, determined by Eq. (11), shows that the transmission is qualitatively the same as we have had for both, the CRIT structures, defined by Eq. (3), and the CRIR structures, defined by Eq. (8). The main difference between all these structures comes from the locations of the perfect transmission and perfect reflection resonances. More specifically, for the case when $\gamma_{\alpha,\beta} \ll |\omega_\alpha - \omega_\beta|$, the Eq. (12) reduces to

$$\omega_r^+ = \omega_\alpha + \frac{\gamma_{\alpha,\beta}}{\omega_\alpha - \omega_\beta}, \quad \omega_r^- = \omega_\beta - \frac{\gamma_{\alpha,\beta}}{\omega_\alpha - \omega_\beta}, \quad (13)$$

and, therefore, the frequency ω_r^- is located very closely to the frequency $\omega_t \equiv \omega_\beta$, leading to a very narrow asymmetric resonant reflection line similar to the CRIR effect discussed above. However, the spectral width of this narrow reflection line, which can be estimated as $\Gamma_r^+ \simeq \gamma_\alpha \gamma_{\alpha,\beta}^2 / (\omega_\alpha - \omega_\beta)^2$, vanishes only when the coupling $\gamma_{\alpha,\beta}$ between the cavities α and β vanishes too. Thus, the Fano-Feshbach resonance in this two-ring structure is hardly tunable, and this is in a sharp contrast to tunability of the line width in the CRIR structures based on photonic-crystal platform and described above.

Moreover, a deeper analysis indicates that the resonant reflection lines in the two-cavity structure can be treated as that of two localized modes of a single compound cavity formed by coupling of two single-mode cavities α and β . When the coupling between cavities α and β vanishes, one of the cavity modes (whose electric field is mostly localized on the cavity β) becomes only weakly coupled to the waveguide, leading to the narrow resonant reflection line in the same way as any weakly coupled cavity mode does. The compound structure of such a mode is responsible for the asymmetric line shape of the Fano resonance which can be employed for various efficient switching devices as discussed in Ref. [29].

6. Photonic structure exhibiting the CRIR effect

As an example of the specific PhC structure exhibiting the CRIR effect, we consider a two-dimensional PhC composed of a triangular lattice of dielectric rods in air. The rods are made of either Si or GaAs ($\epsilon = 12$) with the radius $r = 0.25a$, where a is the lattice spacing. This type of PhC has two large bandgaps for the E-polarized light (i.e. when the electric field is parallel to the rods), and we employ the first gap between the frequencies $\omega a / 2\pi c = 0.2440$ and $\omega a / 2\pi c = 0.3705$.

By reducing the radius of a *single rod*, one can create a monopole-like localized defect mode in this bandgap [see Fig. 3(a,d)]. Reducing the radius of *two neighboring rods* allows to create

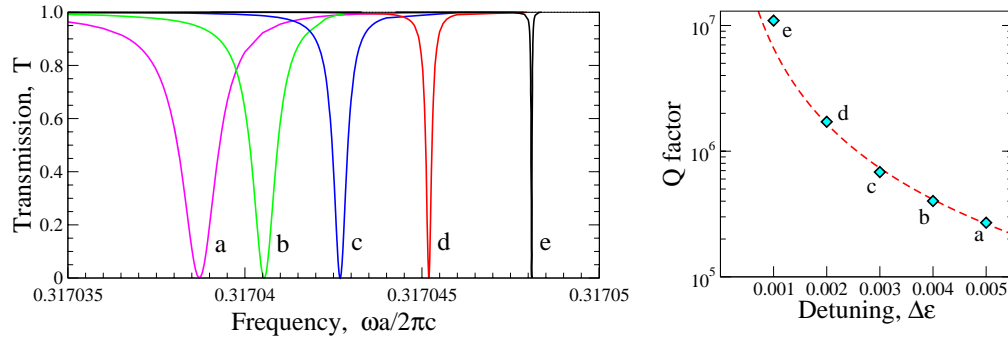


Fig. 5. Width of the asymmetric Fano-Feshbach resonance vs. the permittivity detuning of two cavities. In all cases $\epsilon_\alpha = 12.$, and (a) $\epsilon_\beta = 12.005$, (b) $\epsilon_\beta = 12.004$, (c) $\epsilon_\beta = 12.003$, (d) $\epsilon_\beta = 12.002$, (e) $\epsilon_\beta = 12.001.$.

two localized modes, one with odd and another with even field symmetry [see Fig. 3(b,e,f)]. Removing a row of rods creates the so-called W1-waveguide which guides light with the frequencies $\omega(k)$ determined by the guided mode wave vector k as shown in Fig. 3(c,g). The group velocity $v_g = d\omega/dk$ of the guided mode vanishes at the edge $k = 0$ (with $\omega a/2\pi c = 0.3168$) of the propagation band. At small wave vectors $(ka/2\pi) < 0.1$, it can be approximated as: $v_g/c \approx 1.8155(ka/2\pi) - 0.94776(ka/2\pi)^2$. All numerical results presented in Figs. 3 to 5 are obtained by employing the Wannier functions approach [23] using eleven maximally localized Wannier functions. Good accuracy of these results is confirmed, in particular, by an excellent agreement in Fig. 3 with the results based on the supercell plane-waves calculations [24].

In this paper we consider the CRIR structure made of the W1-waveguide with two side-coupled cavities, each created by reducing the radius of two nearest rods to the value r_{def} . The lines connecting defect rods in each cavity are parallel to the waveguide being separated from the waveguide by three rows of rods, as shown in Fig. 4(a). As we already indicated [see Fig. 3(b,e,f)], such cavities support two localized modes — and, in principle, the CRIR effect can be demonstrated employing any of them. However, to emphasize that the CRIR effect in such a structure survives also in the slow-light regime, we employ the odd-symmetry mode and shift its frequency to the vicinity of the passing band edge $k = 0$ by choosing $r_{\text{def}} = 0.1213a$ for the defect rods in both cavities. For this mode, we should select the bottom sign in expressions “ \pm ” and “ \mp ” in Eqs. (7)–(10). Note that the same odd-symmetry mode has been recently utilized for the slow-light applications of a single-cavity waveguide structure [17].

Figure 4(b) shows the transmission spectra for three structures: with only a single side-coupled cavity (dotted line), with two identical side-coupled cavities (dashed line), and with two slightly different side-coupled cavities (solid line). In the latter case, the difference between cavities is introduced by tuning the dielectric constant of the defect rods in one of the cavities for less than 0.01%. As can be seen, the results of these full-scale calculations completely agree with our analysis based on the approximate discrete model and presented in Sec. 4: as soon as we introduce a small detuning in the properties of the two cavities, there appears a very narrow resonant reflection line at $\omega a/2\pi c \simeq 0.31705$ in addition to the relatively broad resonance at $\omega a/2\pi c \simeq 0.31699$. The corresponding distribution of the electric field at the low-frequency resonance is shown in Fig. 4(a).

In Fig. 5 we plot the transmission spectra of the narrow resonant reflection line and the corresponding resonance quality factors for several values of detuning $\delta\epsilon = \epsilon_\beta - \epsilon_\alpha$ between the dielectric constants of two cavities. Taking into account that for small $\delta\epsilon$ the frequency detuning $\delta\omega$ in Eq. (10) is linearly proportional to $\delta\epsilon$, we expect that the quality factor of this

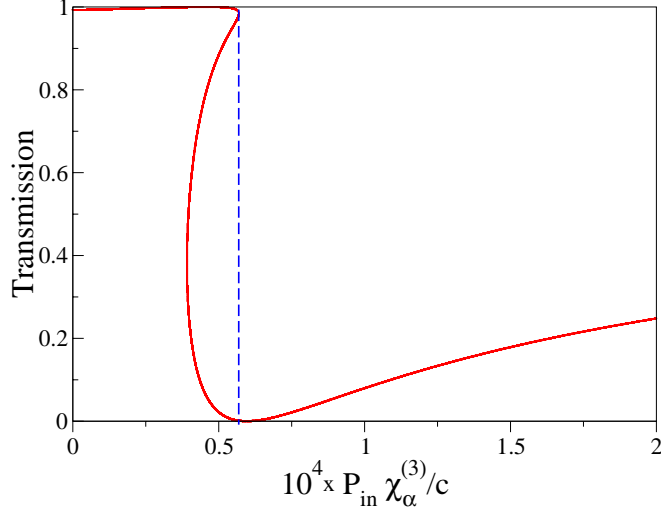


Fig. 6. Nonlinear transmission for the parameters used in Fig. 4. We assume that one cavity is nonlinear, such that $\lambda_\alpha = 3.903 \cdot 10^7 \chi_\alpha^{(3)}$ and $\lambda_\beta = 0$. The light frequency is $\omega = 0.3170418(2\pi c/a)$.

narrow resonance, $Q = \omega_r^\pm / 2\Gamma_r^\pm$, should indefinitely grow as $Q \sim 1/\delta\epsilon^2$ with vanishing of the detuning. As is seen in Fig. 5, the numerical results (see diamonds in the right panel) are in full qualitative agreement with this model prediction (see dashed line in the right panel for the best fit of $Q \sim 1/\delta\epsilon^2$).

7. Nonlinear transmission and all-optical switching

In the *nonlinear* regime, the CRIR structures described here demonstrate low-threshold bistable transmission of light due to the ultra-high Q factor of the asymmetric Fano-Feshbach resonance. For specific example, in Fig. 6 we present the results for the nonlinear transmission of the waveguide-two-cavities structure for the parameters used in Fig. 4 assuming that only one of the cavities is made nonlinear. In this case, choosing the frequency $\omega = 0.3170418(2\pi c/a)$ close to the asymmetric resonance allows achieving a complete 100% switching in the regime of the slow-light propagation. A very similar switching (although, importantly, not in the slow-light regime) can also be achieved in the two-ring photonic [29] or two-cavity photonic crystal structures which we discussed in Sec. 5.

We would like to mention that, to demonstrate the efficiency of the approximations employed in this work, the results for the nonlinear transmission shown in Fig. 6 are obtained by employing the approximate discrete model based on Eq. (6) with the model parameters calculated with the Wannier function approach [23], in contrast to the numerical results presented in Fig. 4–Fig. 5. Using eleven maximally localized Wannier functions, we obtain the following expansions,

$$\omega_{\alpha,\beta} \approx [0.317045 + 6.83 \cdot 10^{-3}(\epsilon_{\alpha,\beta} - 12)](2\pi c/a), \quad (14)$$

and

$$\gamma_{\alpha,\beta}^{(0)} \approx \pm (4.3 \cdot 10^{-6})(2\pi c/a), \quad (15)$$

while the waveguide dispersion in the slow-light regime can be approximated as

$$\omega(k) \approx [0.31680 + 0.89626(ka/2\pi)^2](2\pi c/a). \quad (16)$$

Thus, one of our major finding is that, in a sharp contrast to the CRIT effect, this novel CRIR resonant effect survives also in the slow-light regime and, due to its asymmetric line shape, it allows achieving a 100% all-optical switching of slow light in the nonlinear regime. Currently, the slow-light applications of optical structures based on photonic crystals attract a rapidly growing attention due to the recently achieved experimental success in the observation of slow-light propagation [30, 31, 32, 33]. However, many of the device concepts suggested so far in the physics of photonic crystals cannot be extended to the slow-light regime, and it is important to reveal and analyze novel types of the design concepts which would allow to perform useful operations such as all-optical switching and routing with low group velocities [34, 35, 16, 17]. We therefore believe that the CRIR effect described in this work may be especially useful for elaborated control of slow light, however more extensive studies are beyond the scope of this paper.

8. Conclusions

We have analyzed the resonant transmission of light in a coupled-resonator optical waveguide interacting with two nearly identical cavities, paying a particular attention to differences between the *on-site* and *inter-site* locations of the cavities relative to the waveguide. When two cavities are strongly detuned and associated resonances are well separated [see Fig. 2(b)], both types of photonic-crystal structures are characterized by the similar transmission curves with two distinct Fano resonances. However, when two cavities are only slightly detuned and, therefore, the associated resonances strongly overlap, the on-site and inter-site structures produce quantitatively different transmission curves. Specifically, the on-site geometry shown in Fig. 1(b) may lead to the CRIT effect with a sharp symmetric resonant transmission line [see Fig. 2(c)], while the inter-site geometry shown in Fig. 1(c) may lead to the CRIR effect with a sharp and asymmetric resonant reflection line [see Fig. 2(d)]. The new CRIR transmission we have described here is characterized by a very high and easily tunable quality factor of the reflection line, and this effect differs sharply from the CRIT effect being an all-optical analogue of the electromagnetically-induced transparency demonstrated recently for the structures based on micro-ring resonators. We have demonstrated that the CRIR effect survives also in the slow-light regime and, due to its asymmetric line shape, it allows achieving a 100% all-optical switching of slow light in the nonlinear regime.

It should be noted, however, that in real structures with non-zero optical losses the minimal spectral widths of all resonant reflection and transmission lines in any two-cavity structure considered in this paper cannot be smaller than the line widths determined by the optical losses γ_α^{loss} and γ_β^{loss} at both cavities. Such optical losses can easily be incorporated into the above analysis by replacing $\omega_\alpha \rightarrow \omega_\alpha + i\gamma_\alpha^{loss}$ and $\omega_\beta \rightarrow \omega_\beta + i\gamma_\beta^{loss}$, leading, in particular, to the broadening, $\delta\omega^2/8\gamma_\alpha^{(0)} \rightarrow \delta\omega^2/8\gamma_\alpha^{(0)} + i\gamma_\alpha^{loss}$, of the line widths determined by Eq. (5) as well as Eq. (10).

Acknowledgments

We are grateful to anonymous referees for useful comments. This work has been supported by the Australian Research Council through the Discovery and Center of Excellence research projects.